Saudi Journal of Biological Sciences 28 (2021) 4770–4777

Contents lists available at ScienceDirect

Saudi Journal of Biological Sciences

journal homepage: www.sciencedirect.com

Original article

Early-stage iron deficiency alters physiological processes and iron transporter expression, along with photosynthetic and oxidative damage to sorghum

Sadia Akter Prity [a], Ahmed M. El-Shehawi [b], Mona M. Elseehy [c], Sharaban Tahura [a], Ahmad Humayan Kabir [a,*]

[a] Molecular Plant Physiology Laboratory, Department of Botany, University of Rajshahi, Rajshahi 6205, Bangladesh
[b] Department of Biotechnology, College of Science, Taif University, P.O. Box 11099, Taif 21944, Saudi Arabia
[c] Department of Genetics, Faculty of Agriculture, Alexandria University Alexandria, Egypt

ARTICLE INFO

Article history:
Received 19 February 2021
Revised 27 April 2021
Accepted 28 April 2021
Available online 6 May 2021

Keywords:
Fe deficiency
PS release
Oxidative injury
Strategy II plants

ABSTRACT

Iron (Fe) starvation in Strategy II plants is a major nutritional problem causing severe visual symptoms and yield reductions. This prompted us to investigate the physiological and molecular consequences of Fe deficiency responses at an early stage in sorghum plants. The Fe-starved sorghum did not show shoot biomass reduction, but the root length, biomass, and chlorophyll synthesis were severely affected. The chlorophyll *a* fluorescence analysis showed that the quantum yield efficiency of PSII (Fv/Fm) and photosynthesis performance index (Pi_ABS) in young leaves significantly reduced in response to low Fe. Besides, Fe concentration in root and shoot significantly declined in Fe-starved plants relative to Fe-sufficient plants. Accordingly, this Fe reduction in tissues was accompanied by a marked decrease in PS-release in roots. The qPCR experiment showed the downregulation of *SbDMAS2* (deoxymugineic acid synthase 2), *SbNAS3* (nicotianamine synthase 3), and *SbYSL1* (Fe-phytosiderophore transporter yellow stripe 1) in Fe-deprived roots, suggesting that decreased rhizosphere mobilization of Fe(III)-PS contributes to reduced uptake and long-distance transport of Fe. The *cis*-acting elements of these gene promoters are commonly responsive to abscisic acid and methyl jasmonate, while *SbYSL1* additionally responsive to salicylic acid. Further, antioxidant defense either through metabolites or antioxidant enzymes is not efficient in counteracting oxidative damage in Fe-deprived sorghum. These findings may be beneficial for the improvement of sorghum genotypes sensitive to Fe-deficiency through breeding or transgenic approaches.

1. Introduction

Iron (Fe) deficiency in soil having bicarbonate, high pH, and ferric Fe is a major nutritional disorder in plants (Alcántara et al., 2000). These soil conditions affect the bioavailability of Fe for plants and thus, affect plant growth and yield. As a co-factor, Fe functions in several cellular processes, which include photosynthesis, respiration, and protein formation in plants (Zhang et al., 2019). Photosystem II (PS-II) contains Fe proteins and mislays its efficiency in Fe-deprived plants because of low photosynthetic electron supply (Jiang et al., 2007; Bertamini et al., 2002). As a result, Fe deficiency causes stunned root, leaf chlorosis, and poor maturation in plants (Kabir et al., 2013; Wang et al., 2007).

Sorghum (*Sorghum bicolor*) as a Strategy-II plant possesses a chelation-based Fe uptake system. In the rhizosphere, Strategy-II plants discharge inorganic phytosiderophores (PS) to form Fe-PS complexes resulted in the mobilization of inorganic Fe-III (Vert et al., 2002). Among the chelating molecules associated with Fe-uptake, 2′-deoxymugineic acid (DMA) and nicotianamine synthases (NAS) are the most common in Strategy II plants (Pearce et al., 2014). DMA-related chelation of insoluble Fe increases the solubility and absorption of Fe(III)-DMA in the root system. Barley and wheat secrete a considerable amount of DMA under Fe deficiency (Römheld and Marschner, 1990). The NAS converts three

* Corresponding author.
E-mail address: ahmad.kabir@ru.ac.bd (A.H. Kabir).

Peer review under responsibility of King Saud University.

Production and hosting by Elsevier

https://doi.org/10.1016/j.sjbs.2021.04.092
1319-562X/

molecules of S-adenosyl methionine into NA, which is a Fe chelator involved in Fe transport in plants (Inoue et al., 2003; Higuchi et al., 1995). In other Strategy II plants, *OsDMAS1* and *HvDMAS1* genes have been identified to play roles in DMA synthesis (Kobayashi et al., 2010, Bashir et al., 2006). In addition, higher plants use NAS in the plant cell for chelation and maintenance of Fe homeostasis (Hell and Stephan, 2003). In a transgenic study, tobacco was introduced with the barley *HvNAS1* gene ultimately showed increased Fe and Zn in the shoot (Takahashi et al., 2003). Also, the *YSL* (yellow stripe-like transporter) gene acts as a root transporter of the chelator Fe^{3+}-PS complex (Yordem et al., 2011; Curie et al., 2001).

Fe-deficiency contributes to over-accumulation of reactive oxygen species (ROS), leading to oxidative damages in plant cells (Kabir et al., 2015). However, several antioxidant metabolites and enzymes are often in action to regulate the redox balance, although which is mostly seen in Fe-efficient plant species/cultivars (Kabir et al., 2015; Yang et al., 2015; Ashraf, 2009). Moreover, antioxidant activities in response to stress varied among the plant species, tissues, and subcellular localization (Mittova et al., 2003).

Sorghum is a popular cereal for its importance as grain food, residual crop, and animal feed. Only a few studies reported the responses of Fe-deprived sorghum, but those were solely limited to genotype screening (Obour et al., 2019; Clark et al., 2008). Understanding the responses or consequences of damage due to Fe-deficiency may provide useful knowledge in improving the survivability and yield of sorghum through agronomic or biotechnological approaches. However, Fe-deficiency adversely affects sorghum plants is not yet fully understood. Therefore, we investigated how Fe deficiency lessens growth and development in sorghum plants. Along with the morpho-physiological characterization, a broad range of cellular and molecular responses were studied to determine the mechanistic basis of growth retardation in Fe-deficient sorghum.

2. Materials and methods

2.1. Plant cultivation

The surface of sorghum seeds (var. sucrosorgo 405) was sterilized for 5 min with 70 percent ethanol before placing on moist tissue paper for 3d in a tray at 28 °C. The germinated seedlings were then transferred to solution culture (pH 6.0) supplemented with nutrients (Hoagland and Arnon 1950) as follows (μM): KNO_3 (1600), $Ca(NO_3)_2{\cdot}4H_2O$ (600), KH_2PO_4 (100), $MgSO_4{\cdot}7H_2O$ (200), KCl (50), H_3BO_3 (25), $MnSO_4{\cdot}4H_2O$ (2), $Na_2MoO_4{\cdot}2H_2O$ (0.5) and $CuSO_4{\cdot}5H_2O$ (0.5). The Fe was supplemented as follows: +Fe (25 μM Fe-EDTA) and -Fe (1.0 μM Fe-EDTA). In each plastic container (4L), nine plants were kept at 25 °C with 60% relative and a light intensity of 200 $\mu molm^{-2}\ s^{-1}$ under long-day conditions (14 h light/ 10 h dark) in the growth chamber. The nutrients were replaced every 4d. The plants were cultivated for 14 d before data analysis.

2.2. Characterization of morphological and photosynthetic features

The longest root and shoot were measured by a digital caliper. The dry weight of root and shoot was taken after drying for 3d at 80 °C in an electric oven. The chlorophyll score was measured on young leaves by SPAD meter (Minolta, Japan). Chlorophyll *a* fluorescence kinetics (OJIP) such as Fv / Fm (photosystem II quantitative efficiency) and Pi ABS (photosynthesis index), were also measured by FluorPen 100 (photon systems instruments, Czech Republic) in dark-adapted young leaves for 1 h.

2.3. Analysis of Fe concentration

Tomato root specimens were washed once with 0.1 mM $CaSO_4$ and rinsed multiple times with Milli-Q water to remove the surface contaminants. Roots and shoots were dried separately in the oven at 70 °C for 72 h. Dry samples were then weighed and dissolved with $HClO_4/HNO_3$, 1:3 v/v. The concentration of Fe in the digestion solution was determined by atomic absorption spectroscopy (AA-6800, Shimadzu, Japan).

2.4. Determination of the release of PS in roots

The PS secretion in roots was analyzed as described earlier (Khobra and Singh, 2018). Briefly, entire plants were submerged in a pump-aerated beaker containing 1 N NaOH and 4 mM $FeCl_3$ for 3 h. The solution was then filtered through Whatman filter paper (grade: 1, diameter: 125 mm, Merck, India) to eliminate the degradation of the microbes. The Fe(III) was then reduced by adding 8 percent hydroxylaminochloride at 55 °C for 20 min. Subsequently, 10 mM ferrozine and 0.5 M Na-acetate buffer (pH 4.6) were added prior to absorbance monitoring of the solution (Fe^{3+} ion) at 562 nm.

2.5. Expression pattern of candidate genes and promoter analysis

The total RNA in roots was extracted using SV RNA extraction system (Promega, USA). The quantified RNA was then converted to cDNA using the reverse-transcription system before PCR analysis in an Eco™ real-time PCR system (Illumina, USA) using gene-specific primers for *SbDMAS2, SbNAS3 and SbYSL1* genes (Supplementary Table S1). The PCR reactions were set as follows: 95 °C for 3 min, followed by 40 cycles at 95 °C for 10 sec, 57 °C for 30 sec. The relative expression of candidate genes was calculated by the dd − ΔCt method (Livak and Schmittgen, 2001) considered *Actin* as an internal control. The qPCR experiment was repeated three times. Besides, the PlantCare web tool was used for scanning the *cis*-elements present in promoter regions of *SbDMAS2, SbNAS3 and SbYSL1* promoters (Lescot et al., 2002).

2.6. Analysis of stress indicators

Bovine serum albumin (BSA) curve was plotted to estimate the total soluble protein by Bradford assay (Guy et al., 1992). In short, fresh root and shoot sample protein extraction were performed by grinding with Tris-HCl buffer (50 mM, pH 7.5), 0.04% (v / v) β-mercaptoethanol, and 2 mM EDTA. The crude samples were centrifuged at 12000 rpm for 10 min before collecting the transparent fluid portion. Finally, 1 ml of Coomassie Brilliant Blue (CBB) was added to the supernatant before measuring the absorbance at 595 nm.

The loss of cell membrane integrity was measured by a conductivity meter in both root and shoot (Lutts et al., 1996). Briefly, root and shoot surface components were washed with deionized water. The fresh specimens were then transferred to a deionized water beaker (20 ml) and incubated at 25 °C for 2 h. Afterward, the solution's electrical conductivity (EC1) was calculated. The samples were then heated in a water bath for 20 min at 95 °C to ensure the maximum release of electrolytes and then cooled down to 25 °C. The final EC (EC2) was then recorded and determined as follows: = (EC1/EC2) × 100 (%).

Evans blue method was used to determine the rate of cell death in the root and shoot (Zhao et al., 2005). The entire fresh root and shoot were transferred 2 ml of Evan's blue mixture and waited 15 min. The suspension was subsequently dried up to 10 min in 1 ml of 80% ethanol. The tubes with solutions were then incubated in a water bath for 15 min at 50 °C and then centrifuged for 10 min

at 12000 rpm. The absorbance of the supernatant was measured at 600 nm. Finally, the percentage of cell death was evaluated based on sample fresh weight.

2.7. Estimation of H_2O_2 and O_2^-

The root and shoot samples were homogenized in 0.1% trichloroacetic acid (Alexieva et al., 2001). The extracts were then centrifuged at 10,000 rpm for 15 min. The top aqueous segment was mixed with 10 mM potassium phosphate (pH 7.0), 1 M KI, and placed in a dark room to allow reaction for 1 h. Finally, the absorbance of the solution was read at 390 nm. Besides, the superoxide (O_2^-) was calculated using a coefficient of extinction 2.16 × 104 $M^{-1}{\cdot}cm^{-1}$), as described by Hu et al. (2012). Briefly, the fresh samples were washed with water, homogenized with chilled K-phosphate buffer (10 mM), and centrifuged at 12000 rpm at 4 °C for 10 min. The clear supernatant was mixed with an assay solution containing 0.5 mM XTT sodium salt and 50 mM Tris-HCl (pH 7.5). Finally, the solution's optical density was read at 580 nm.

2.8. Analysis of antioxidant enzymes

Briefly, plant root and shoot were independently homogenized in mortar pestle with 100 mM phosphate buffer (pH 7.0). The homogenate was centrifuged for 10 min at 8000 rpm, and the transparent part was collected for further analysis. The 100 μL plant extract was added with 0.1 mM EDTA, 50 mM $NaHCO_3$ (pH 9.8), and 0.6 mM epinephrine for the determination of SOD activity (Goud and Kachole, 2012). After 4 min, the confirmation of adrenochrome was read at 475 nm. For ascorbate peroxidase (APX) activity, 0.1 mM EDTA, 50 mM potassium phosphate buffer (pH 7.0), 0.1 mM H_2O_2, and 0.5 mM ascorbic acid were added to 100 μL extract (Sun and Zigman, 1978). Afterward, the absorbance was recorded at 290 nm and APX activity was calculated based on the extinction coefficient (2.8 mM^{-1} cm^{-1}). The catalase (CAT) activity was analyzed by mixing 100 μL plant extract with 100 mM MKP-buffer (adjusted pH 7.0), 6% hydrogen peroxide. Finally, the absorption of the solution was reported at 240 nm in 30 sec to 1 min interval (extinction coefficient 0.036 mM^{-1} cm^{-1}). In addition, 100 μL of extract was added to 0.2 M KP-buffer (pH 7.0), 1 mM EDTA, 0.2 mM NADPH and 20 mM oxidized glutathione (GSSG) for (glutathione reductase) GR analysis. The absorbance of the solution was read at 340 nm. Finally, the GR activity was calculated using the extinction coefficient (6.12 mM^{-1} cm^{-1}) as described earlier (Halliwell and Foyer, 1978).

2.9. Analysis of S-metabolites

Briefly, plant samples were washed with ultra-pure water and then dried in an oven. The samples were pulverized using a milling machine into a fine powder. The samples were then dissolved with 50% methanol and filtered using Whatman filter paper (grade: 1, diameter: 125 mm, Merck, India). We analyzed the amino acid in root and shoot with dual-wavelength (280 and 360 nm) by Waters 2489 high-performance liquid chromatography (HPLC) in C18 reverse-phase column (Kabir et al., 2016). We maintained gradient conditions (pore size: 300 A, particle size: 5 μm, pH Range: 1.5–10, Dimension: 250 mm × 10 mm; column oven temperature: 250 °C, flow rate: 1.0 ml/min, run time: 45 min) using 100% acetonitrile as the mobile phase (Kabir et al., 2016). The samples were diluted (100 ×) and then filtered (0.22 μm Minisart Syringe Filters) before injection (20 μL).

2.10. Statistical analysis

In this study, each experiment was repeated three times for consistency in plants cultivated in a randomized block design. The significance of the mean of replications was assessed by *t*-test using Microsoft Excel 2007 at a 5% significance level. In preparing graphical figures, GraphPad Prism 6 was used.

3. Results

3.1. Plant growth, photosynthesis efficiency, and Fe concentration

Fe starvation induced a significant reduction in root length and dry weight in contrast to Fe-sufficient controls (Fig. 1a–c). However, shoot height and dry weight did not show any significant changes following Fe shortage compared to Fe-sufficient plants (Fig. 1a–c). The SPAD score, an indicator of chlorophyll synthesis, was significantly reduced in young leaves under Fe starvation than in the controls (Fig. 2a). Further, the Fv/Fm value of the Fe-sufficient sorghum was found to be above 0.8, while Fe-starved plants showed a significant decline in Fv/Fm (below 0.6) value (Fig. 2b). Similarly, Pi_ABS value showed a significant reduction under Fe-deficiency in young leaves compared to plants cultivated with sufficient Fe (Fig. 2c).

3.2. Fe concentration, PS release and gene expression

The root and shoot Fe concentration of sorghum plants decreased considerably under low Fe supplement compared to plants cultivated with sufficient Fe in the hydroponic culture (Fig. 3a). PS release from the roots remarkably decreased in Fe-starved sorghum in contrast to Fe-adequate plants (Fig. 3b). We have analyzed the relative transcript levels in the roots of the sorghum of key Fe-acquisition genes. Plants exposed to Fe starvation exhibited a significant downregulation of *SbDMAS1*, *SbNAS1,* and *SbYSL1* genes in roots relative to Fe-adequate conditions (Fig. 3c).

The significant *cis*-acting elements in these gene promoters were ABRE (*cis*-acting element involved in the abscisic acid responsiveness), CGTCA-motif (*cis*-acting regulatory element involved in the methyl jasmonate-responsiveness), G-Box (*cis*-acting regulatory element involved in light responsiveness), O_2-site (*cis*-acting regulatory element involved in zein metabolism regulation), TGACG-motif (*cis*-acting regulatory element involved in the methyl jasmonate -responsiveness), GCN4_motif (*cis*-regulatory element involved in endosperm expression), LTR (*cis*-acting element involved in low-temperature responsiveness), motif I (*cis*-acting regulatory element root-specific), AuxRR-core (*cis*-acting regulatory element involved in auxin responsiveness), CAT-box (*cis*-acting regulatory element related to meristem expression), MSA-like (*cis*-acting element involved in cell cycle regulation), TCA-element (*cis*-acting element involved in salicylic acid responsiveness) as analyzed by PlantCare (Table 1).

3.3. Changes in stress indicators

Fe deficiency showed a significant decline in total soluble protein in root and shoot of sorghum relative to Fe-sufficient plants (Fig. 4a). In addition, electrolyte leakage in roots increased dramatically in contrast to controls due to Fe starvation. However, this phenomenon did not vary in the shoot of sorghum between Fe adequate and Fe-deficient conditions (Fig. 4b). Besides, cell death (%) in both root and shoot remarkably increased following Fe-deficiency in contrast to Fe-sufficient controls (Fig. 4c).

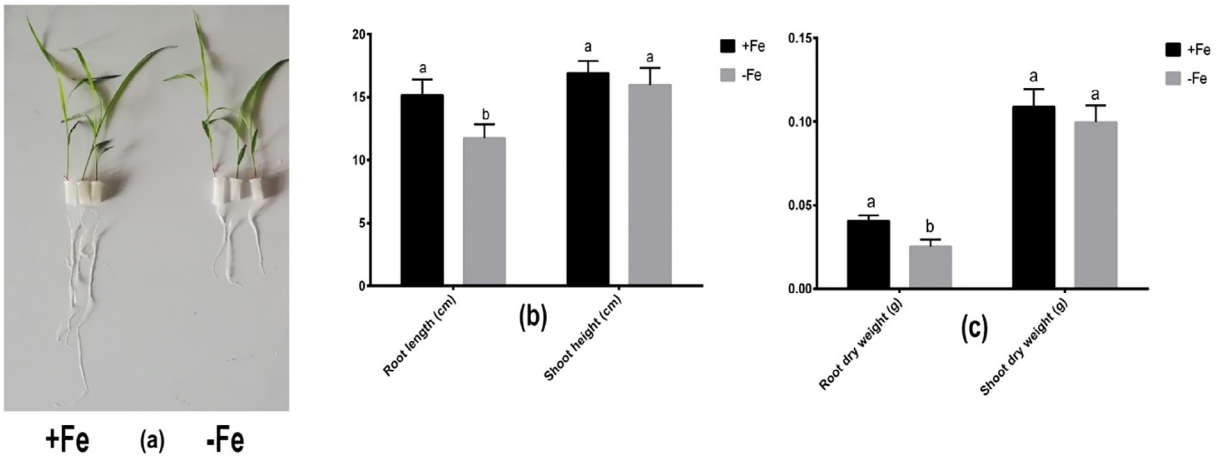

Fig. 1. Plant phenotype (a), tissue length (b) and dry weight (c) of 14d-old sorghum plants cultivated in Fe-sufficient and Fe-deficient conditions. Different letters in Fig. (c) and (d) indicate significant differences between means ± SD of treatments (n = 3) at a P < 0.05 significance level.

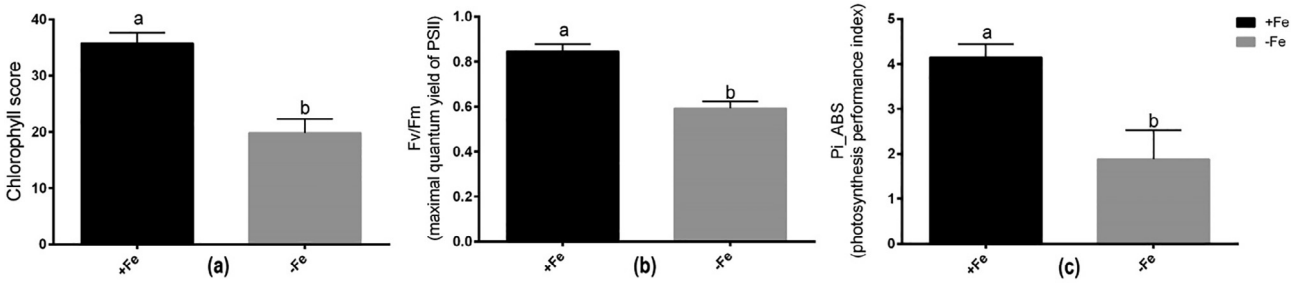

Fig. 2. SPAD score (a), Fv/Fm (b) and Pi_ABS (c) in leaves of 14d-old sorghum plants in Fe-sufficient and Fe-deficient conditions. Different letters indicate significant differences between means ± SD of treatments (n = 3) at a P < 0.05 significance level.

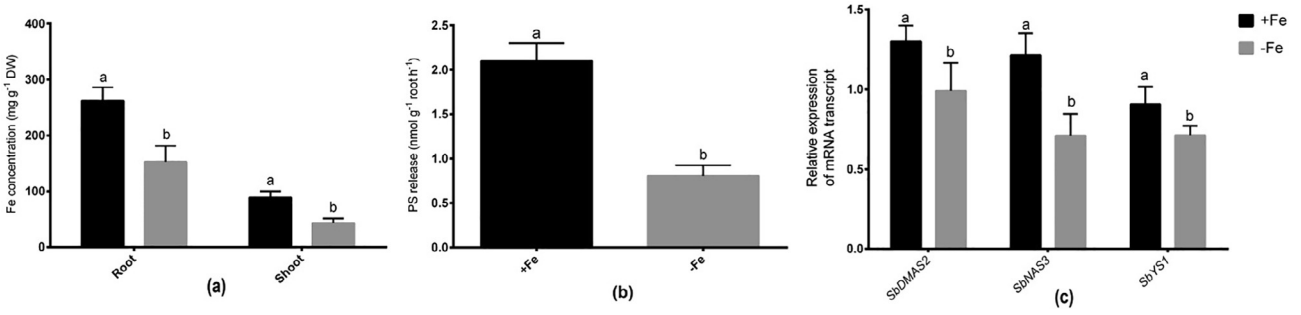

Fig. 3. Tissue Fe concentration (a), PS release (b) and expression of candidate genes (c) in roots of 14d-old sorghum plants cultivated in Fe-sufficient and Fe-deficient conditions in 14d-old sorghum plants. Different letters indicate significant differences between means ± SD of treatments (n = 3) at a P < 0.05 significance level.

Table 1
Cis-regulatory element analysis of *SbDMAS2*, *SbNAS3* and *SbYSL1* gene promoters.

Gene promoters	ABRE	CAAT-box	CGTCA-motif	G-Box	O_2-site	TGACG-motif	GCN4_motif	LTR	motif I	AuxRR-core	CAT-box	MSA-like	TCA-element
SbDMAS2	3	4	3	4	1	3							
SbNAS3	4	2	4	6		4	1	1	1				
SbYSL1	5	8	4	6	1			2		2	1	1	1

ABRE (*cis*-acting element involved in the abscisic acid responsiveness), CAAT-box (common *cis*-acting element in promoter and enhancer regions), CGTCA-motif (*cis*-acting regulatory element involved in the methyl jasmonate -responsiveness), G-Box (*cis*-acting regulatory element involved in light responsiveness), O_2-site (*cis*-acting regulatory element involved in zein metabolism regulation), TGACG-motif (*cis*-acting regulatory element involved in the methyl jasmonate -responsiveness), GCN4_motif (*cis*-regulatory element involved in endosperm expression), LTR (*cis*-acting element involved in low-temperature responsiveness), motif I (*cis*-acting regulatory element root specific), AuxRR-core (*cis*-acting regulatory element involved in auxin responsiveness), CAT-box (*cis*-acting regulatory element related to meristem expression), MSA-like (*cis*-acting element involved in cell cycle regulation), TCA-element (*cis*-acting element involved in salicylic acid responsiveness)

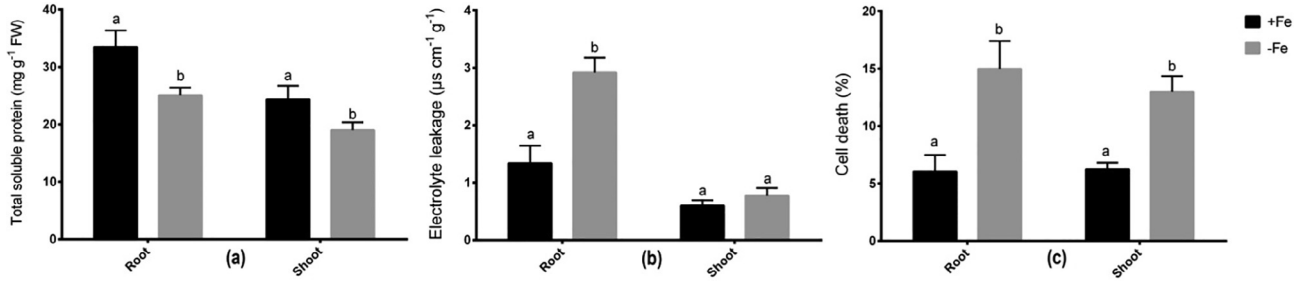

Fig. 4. Changes in different stress indicators in root and shoot of sorghum cultivated in Fe-sufficient and Fe-deficient conditions in 14d-old sorghum plants. Different letters in each column indicate significant differences between means ± SD of treatments (n = 3) at a P < 0.05 significance level.

3.4. Reactive oxygen species

Compared to Fe-adequate plants, the H_2O_2 concentration was significantly induced in the roots of Fe-starved sorghum (Fig. 5a). However, Fe-starvation caused no significant changes in H_2O_2 concentration in the shoot in comparison with Fe-sufficient controls (Fig. 5a). Further, the reactive O_2^- in root and shoot significantly increased due to Fe-deficiency relative to Fe-sufficient plants (Fig. 5b).

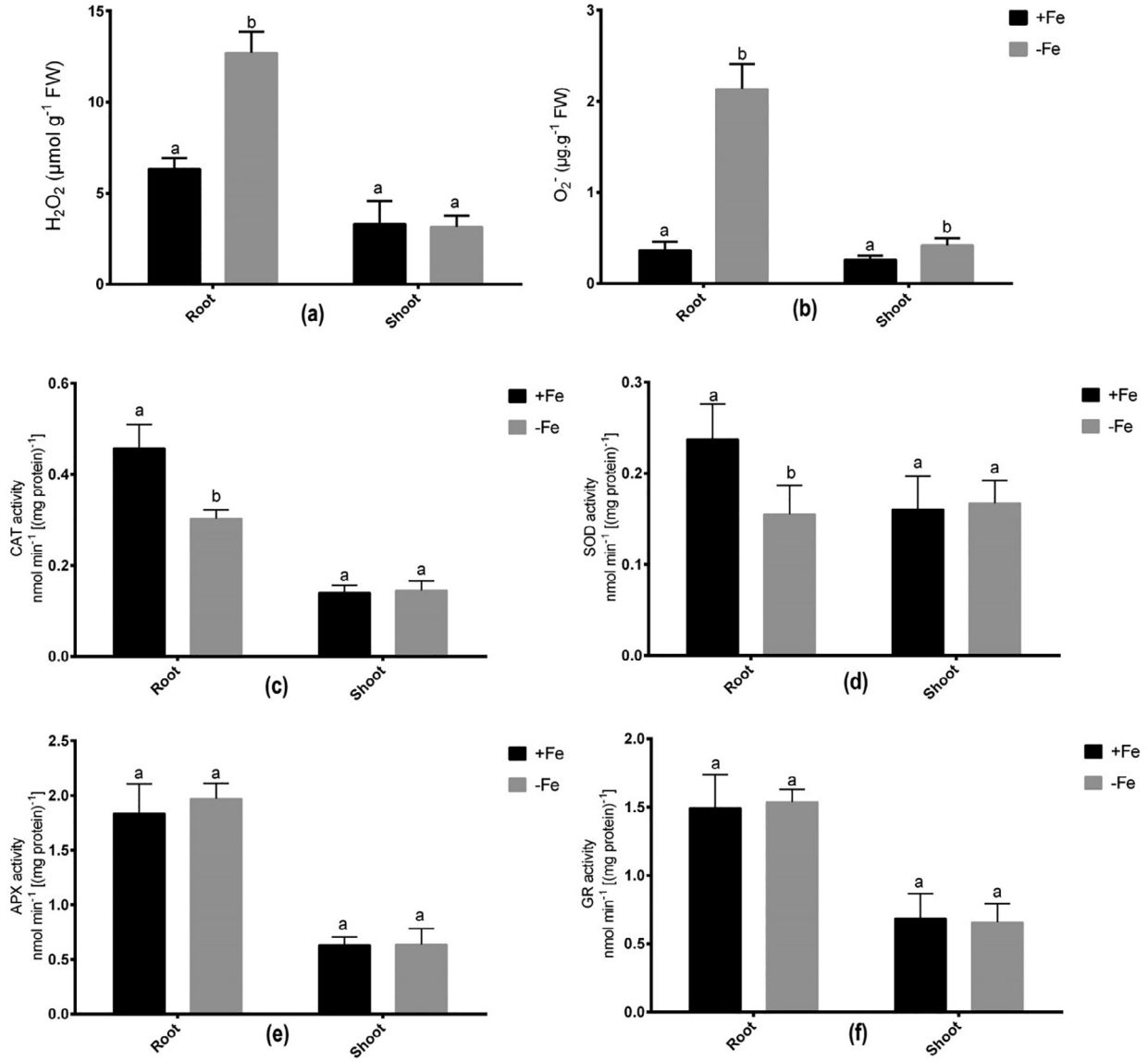

Fig. 5. Changes in ROS molecules and different antioxidant enzymes in root and shoot of sorghum cultivated in Fe-sufficient and Fe-deficient conditions in 14d-old sorghum plants. Different letters indicate significant differences between means ± SD of treatments (n = 3) at a P < 0.05 significance level.

3.5. Antioxidant enzymes

In this study, the CAT and SOD activities showed a substantial decline in the root but not in the shoot in Fe-deprived plants relative to controls (Fig. 5c and d). Nevertheless, Fe-shortage did not show any effect on APX and GR activities in root and shoot subjected to Fe-shortage in contrast to Fe-adequate plants (Fig. 5e and f).

3.6. Relative changes in S-metabolites

In this study, cysteine and methionine significantly declined in the root, although none of the amino acids did vary in shoot under Fe-starvation in contrast to Fe-sufficient plants (Fig. 6a and b). However, glutathione concentration in root or shoot did not vary following Fe deficiency relative to Fe-sufficient conditions (Fig. 6c).

4. Discussion

4.1. Plant growth and photosynthesis under Fe deficiency

This study explores our understanding of how Fe-deficient sorghum plants respond at an early stage. Induction of Fe deficiency caused severe growth retardation in the roots, although the shoot biomass and length were not affected. It may be possible that the shoot was not affected due to a short growth period, which is also observed in sorghum previously (Hirai et al., 2007). Along with the visual leaf symptoms, the SPAD score dramatically dropped due to Fe starvation, suggesting the occurrence of photosynthesis efficiency in sorghum leaves. To further confirm it, Chl *a* fluorescence analysis consistently showed the decrease in *Fv*/*Fm* value in leaves. It actively supports the diagnosis of Fe-deficiency symptoms and suggests the reduction in quantum yield efficiency in Fe-deprived sorghum. The decrease in the quantum yield of PSII is often associated with the Fe-deficient leaves (Abadía et al., 1999). Further, Pi_ABS was also consistently declined in Fe-deprived leaf of sorghum, which might be linked to the low energy conservation efficiency index by PS-II antenna. In C4 plants, mesophyll and bundle sheath cells are mostly affected by Fe deficiency (Stocking, 1975). However, PSI is more sensitive than PSII as it contains several Fe atoms. As PSI activity gets arrested, the PSII center functions, adjusting the reduced efficiency of PSI to transport the electrons to ferredoxin (Sharma, 2007). Several studies documented that a chlorotic leaf is closely correlated with PSII efficacy in Fe-deprived plants (Gogorcena et al., 2001; Donnini et al., 2003). However, this relation may vary depending on the plant species and mineral deficiency. Under Mn deficiency, barley plants showed a decrease in PSII activity, although the chlorophyll was stable in leaves (Schmidt et al., 2013). Our findings indicate that Fe-starvation triggers the changes in PS-II activity that is directly related to the reaction center or various energy transfer pathways in sorghum leaves. This message can be useful to strengthen the knowledge to avoid damage to the photosynthetic apparatus in Fe-starved sorghum.

4.2. Changes in Fe concentration and transporter genes

The Fv/Fm value near 0.8 in healthy plants is usually considered safe for non-stress conditions. Hence, chlorophyll *a* fluorescence is a popular strategy to study photosynthetic systems in stress-induced plants (Baker and Rosenqvist, 2004). In this study, the relationship between quantum yield efficiency and tissue Fe was further evaluated. The Fe concentration was severely decreased under Fe starvation in sorghum. Although the root morphology is consistent with root Fe concentration, the shoot biomass did not change owing to Fe starvation. However, the chlorophyll and PSII status clearly states that Fe-deficiency does not appear to inhibit the development of aerial parts but is closely linked to photosynthetic kinetics in sorghum.

Alternation in Fe uptake, which is another spotlight of the study, was accompanied by the decreased release of PS in Fe-starved sorghum. PS possesses a chelation affinity for Fe(III) in Strategy II plants, allowing high Fe flow into the roots (Inoue et al., 2009; Curie et al., 2001). In this study, we noticed a substantial decrease of PS release in roots following Fe-deficiency in sorghum. Khobra and Singh (2018) demonstrated that Fe-efficiency was accompanied by higher PS release relative to the wheat lines inefficient to cope with Fe-deprivation (Khobra and Singh, 2018). The release of PS is dependent on plant Fe status as Fe is involved with the deactivation or activation of organic ligands (Mimmo et al., 2014).

We also studied the expression of transporter genes typically found in plants within Strategy II relating to Fe uptake and PS release under Fe-deficiency. In this study, the substantial decrease of *SbDMAS2*, *SbNAS3,* and *SbYSL1* in Fe-deprived roots implies that Fe uptake and bioavailability in the rhizosphere were severely affected by Fe shortage resulting in stunted growth and physiological damages in sorghum plants. These results on the transporter genes in sorghum are contradictory to a few Strategy II plant species. In wheat, *DMAS* and *YSL* homologs were also up-regulated on iron hunger (Wang et al., 2019). However, it is known that sorghum exhibits different substrate specificity and expression patterns of transporters than barley and maize subjected to Fe deficiency (Hirai et al., 2007). In rice, NA transporters were induced under iron deficiency in the root epidermis (Inoue et al., 2008). It is widely known that *YSL* transporters are associated with the transport of Fe from root to shoot in Strategy II plants (Koike et al., 2004; Curie et al., 2001). In barley, *HvNAS1* and *HvTOM1* genes sharply induced after Fe deficiency resulted in Fe utilization and redistribution within the shoot (Nikolic et al., 2019). However, based on our finding, it appears that Fe availability in the rhizosphere is largely affected due to the downregulation of *SbDMAS2, SbNAS3,* and

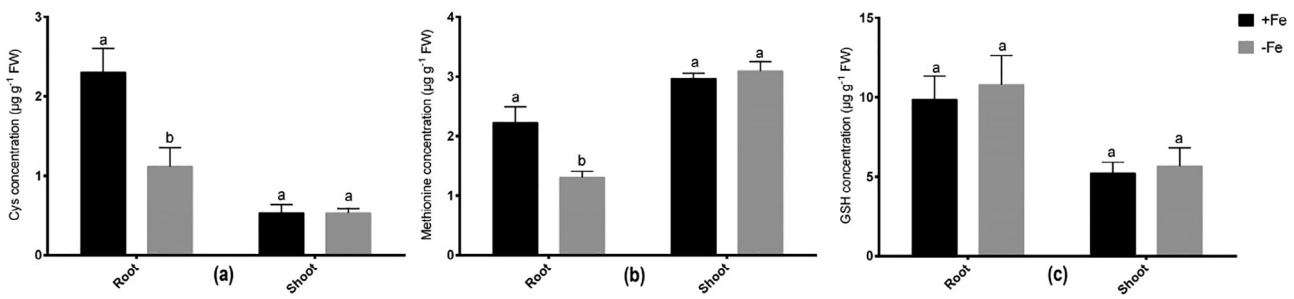

Fig. 6. Changes in S-metabolites in root and shoot of sorghum cultivated in Fe-sufficient and Fe-deficient conditions in 14d-old sorghum plants. Different letters indicate significant differences between means ± SD of treatments (n = 3) at a $P < 0.05$ significance level.

SbYSL1-mediated decreased transportation of Fe to the aerial part in Fe-starved sorghum. This coincides with chlorosis and PS-II damage in Fe-starved sorghum. It is also known that strategies to overcome Fe-deficiency symptoms are highly genotype-specific. Besides, promoter analysis reveals the involvement of *cis*-acting elements associated with several stress-responsive elements, such as abscisic acid, methyl jasmonate and salicylic acid. Studies reported that methyl jasmonate signaling is involved in the expression of Fe-deficiency induced genes in plants (Kobayashi et al., 2016), while salicylic acid signaling trigger transcriptional regulation of downstream Fe-related genes (Zuchi et al., 2015).

4.3. Redox status and antioxidant properties

Photo-oxidative damage is often observed in Fe-deficient plants. Plants starving with Fe are more prone to oxidative stress as Fe is a co-factor of many antioxidant enzymes. In this study, none of the S-metabolites were found to be induced due to Fe shortage in sorghum, indicating that the Fe status of the plant may also be linked to the S status of the sorghum plants. In maize, Fe deficiency caused excess Zn and thiol accumulation along with growth reduction (Kanai et al., et al., 2009). S-induced physiological and antioxidant activities are commonly seen in Fe-starved plants (Zuchi et al., 2009). In plants, chloroplast and photosystem machinery is closely linked with the involvement of Fe-S proteins (Forieri et al., 2013; Vigani et al., 2009). Additionally, many enzymes involved in S assimilation include Fe. Besides, the accumulation of S is frequently related to the accumulation of Met, the forerunner of PS (Luna et al., 2018). Further, CAT and SOD activity severely affected following Fe deficiency in sorghum. The relation of Fe shortage with decreased SOD activity in Arabidopsis was reported (Ramírez et al., 2013). Whether Fe deficiency impairs ROS balance in Strategy II plants is still not adequately studied. However, some evidence has been published on the association of low Fe availability and reduced activities of SOD and APX in sunflower and Arabidopsis (Ramírez et al., 2013; Ranieri et al., 2000). However, APX and GR showed no induction in sorghum tissues subjected to Fe-starvation, suggesting that inefficiency to mitigate excess ROS is possibly related to the damage of chloroplasts and cellular proteins. However, the ROS regulation in plant cells may vary on the species and cultivar of species.

5. Conclusion

This research offers essential knowledge on the mechanistic basis of Fe-starvation in sorghum. Fe shortage caused stunned growth, photosynthetic inefficiency, and cellular damage in sorghum. The substantial decrease of Fe in tissues was mostly dependent on PS-mediated Fe mobilization accompanied by the downregulation of PS-related genes in sorghum roots. Besides, *in silico* analysis revealed the presence of *cis*-regulatory elements in promoters associated with several stress-responsive elements, such as methyl jasmonate and salicylic acid. Furthermore, antioxidant defense neither by S-metabolites or antioxidant enzymes AMF assisted Fe-deprived sorghum plants in overcoming oxidizing injuries. These results provide the necessary context for reducing Fe-deficiency symptoms in sorghum or other Strategy II plants.

Declaration of Competing Interest

The authors declare that they have no known competing financial interests or personal relationships that could have appeared to influence the work reported in this paper.

Acknowledgment

We are thankful to the Central Science Laboratory of Rajshahi University.

Funding statement

The current work was funded by Taif University Researchers Supporting Project number (TURSP - 2020/75), Taif University, Taif, Saudi Arabia.

Appendix A. Supplementary data

Supplementary data to this article can be found online at https://doi.org/10.1016/j.sjbs.2021.04.092.

References

Abadía, J., Morales, F., Abadia, A., 1999. Photosystem II efficiency in low chlorophyll, iron-deficient leaves. Rec. Prog. Plant Nutr. 215 (2), 183–192.
Alcántara, E., Romera, F., Canete, M., De la Guardia, M., 2000. Effects of bicarbonate and iron supply on Fe (III) reducing capacity of roots and leaf chlorosis of the susceptible peach rootstock "Nemaguard". J. Plant Nutr. 23, 1607–1617.
Alexieva, V., Sergiev, I., Mapelli, S., Karanov, E., 2001. The effect of drought and ultraviolet radiation on growth and stress markers in pea and wheat. Plant Cell Environ. 24, 1337–1344.
Ashraf, M., 2009. Biotechnological approach of improving plant salt tolerance using antioxidants as markers. Biotechnol. Adv. 27, 84–93.
Baker, N.R., Rosenqvist, E., 2004. Applications of chlorophyll fluorescence can improve crop production strategies: an examination of future possibilities. J. Exp. Bot. 55, 1607–1621.
Bashir, K., Inoue, H., Nagasaka, S., Takahashi, M., Nakanishi, H., Mori, S., Nishizawa, N.K., 2006. Cloning and characterization of deoxymugineic acid synthase genes from graminaceous plants. J. Biol. Chem. 281, 32395–32402.
Bertamini, M., Muthuchelian, K., Nedunchezhian, N., 2002. Iron deficiency induced changes on the donor side of PS II in field grown grapevine (*Vitis vinifera* L. cv. Pinot noir) leaves. Plant Sci. 162, 599–605.
Clark, R.B., Yusuf, Y., Ross, W.M., Maranville, J.W., 2008. Screening for sorghum genotypic differences to iron deficiency. J. Plant Nutri. 5, 587–604.
Curie, C., Panaviene, Z., Loulergue, C., Dellaporta, S.L., Briat, J.F., Walker, E.L., 2001. Maize yellow stripe1 encodes a membrane protein directly involved in Fe (III) uptake. Nature 409, 346.
Donnini, S., Castagna, A., Guidi, L., Zoechi, G., Ranieri, A., 2003. Leaf responses to reduced iron availability in two tomato genotypes: T3238FER (iron efficient) and T3238fer (iron inefficient). J. Plant Nutr. 26, 2137–2148.
Forieri, I., Wirtz, M., Hell, R., 2013. Toward new perspectives on the interaction of iron and sulfur metabolism in plants. Front. Plant Sci. 4, 357.
Gogorcena, Y., Molias, N., Larbi, A., Abadía, J., Abadía, A., 2001. Characterization of the responses of cork oak (*Quercus suber*) to iron deficiency. Tree Physiol. 21, 1335–1340.
Goud, P.B., Kachole, M.S., 2012. Antioxidant enzyme changes in neem, pigeonpea and mulberry leaves in two stages of maturity. Plant Signal. Behav. 7, 1258–1262.
Guy, C., Haskell, D., Neven, L., Klein, P., Smelser, C., 1992. Hydration-state-responsive protein link cold and drought stress in spinach. Planta 188, 265–270.
Halliwell, B., Foyer, C.H., 1978. Properties and physiological function of a glutathion reductase purified from spinach leaves by affinity chromatography. Planta 139, 9–17.
Hell, R., Stephan, U.W., 2003. Iron uptake, trafficking and homeostasis in plants. Planta 216, 541–551.
Hoagland, D.R., Arnon, D.I., 1950. The water-culture method for growing plants without soil. Circ. Cali. Agric. Exp Stat 347.
Higuchi, K., Nishizawa, N.K., Yamaguchi, H., Römheld, H., Marschner, H., Mori, S., 1995. Response of nicotianamine synthase activity to Fe-deficiency in tobacco plants as compared with barley. J. Exp. Bot. 46, 1061–1063.
Hirai, M.H., Higuchi, K., Sasaki, H., Suzuki, T., Maruyama, T., Yoshiba, M., Tadano, T., 2007. Contribution of iron associated with high-molecular-weight substances to the maintenance of the SPAD value of young leaves of barley under iron-deficient conditions. Soil Sci. Plant Nutr. 53, 612–620.
Hu, L., Li, H., Pang, H., Fu, J., 2012. Responses of antioxidant gene, protein and enzymes to salinity stress in two genotypes of perennial ryegrass (*Lolium perenne*) differing in salt tolerance. J. Plant Physiol. 169 (2), 146–156.
Inoue, H., Kobayashi, T., Nozoye, T., Takahashi, M., Kakei, Y., Suzuki, K., Nakazono, M., Nakanishi, H., Mori, S., Nishizaya, N.K., 2009. Rice *OsYSL15* is an iron-regulated iron (III)-deoxymugineic acid transporter expressed in the roots and is essential for iron uptake in early growth of the seedlings. J. Biol. Chem. 284, 3470–3479.
Inoue, H., Takahashi, M., Kobayashi, T., Suzuki, M., Nakanishi, H., Mori, S., Nishizawa, N.K., 2008. Identification and localisation of the rice nicotianamine

aminotransferase gene OsNAAT1 expression suggests the site of phytosiderophore synthesis in rice. Plant Mol. Biol. 66, 193–203.
Inoue, H., Higuchi, K., Takahashi, M., Nakanishi, H., Mori, S., Nishizawa, N.K., 2003. Three rice nicotianamine synthase genes, OsNAS1, OsNAS2, and OsNAS3 are expressed in cells involved in long-distance transport of iron and differentially regulated by iron. Plant J. 36, 366–381.
Jiang, C., Gao, H., Zou, Q., Shi, L., 2007. Effects of iron deficiency on photosynthesis and photosystem II function in soybean leaf. J. Plant Physiol. Mol. Biol. 33, 53–60.
Kobayashi, T., Itai, R.N., Senoura, T., Oikawa, T., Ishimaru, Y., Ueda, M., Nakanishi, H., Nishizawa, N.K., 2016. Jasmonate signaling is activated in the very early stages of iron deficiency responses in rice roots. Plant Mol. Biol. 91 (4–5), 533–547.
Kabir, A.H., Paltridge, N.G., Roessner, U., Stangoulis, J.C., 2013. Mechanisms associated with Fe-deficiency tolerance and signaling in shoots of *Pisum sativum*. Physiol. Plant. 147, 381–395.
Kabir, A.H., Rahman, M.M., Haider, S.A., Paul, N.K., 2015. Mechanisms associated with differential tolerance to Fe deficiency in okra (*Abelmoschus esculentus* Moench) Environ. Exp. Bot. 112, 16–26.
Kabir, A.H., Begum, M.C., Haque, A., Amin, R., Swaraz, A.M., Haider, S.A., Paul, N.K., Hossain, M.M., 2016. Genetic variation in Fe toxicity tolerance is associated with the regulation of translocation and chelation of iron along with antioxidant defence in shoots of rice. Funct. Plant Biol. 43 (11), 1070–1081.
Kanai, M., Hirai, M., Yoshiba, M., Tadano, T., Higuchi, K., 2009. Iron deficiency causes zinc excess in *Zea mays*. Soil Sci. Plant Nutr. 55, 271–276.
Khobra, R., Singh, B., 2018. Phytosiderophore release in relation to multiple micronutrient metal deficiency in wheat. J. Plant Nutr. 41, 679–688.
Kobayashi, T., Nakanishi, H., Nishizawa, N.K., 2010. Recent insights into iron homeostasis and their application in graminaceous crops. Proceed. Jap. Acad. 86, 900–913.
Koike, S., Inoue, H., Mizuno, D., Takahashi, M., Nakanishi, H., Mori, S., Nishizawa, N. K., 2004. *OsYSL2* is a rice metal-nicotianamine transporter that is regulated by iron and expressed in the phloem. Plant J. 39, 415–424.
Lescot, M., Déhais, P., Thijs, G., Marchal, K., Moreau, Y., Van de Peer, Y., Rouzé, P., Rombauts, S., 2002. PlantCARE, a database of plant cis-acting regulatory elements and a portal to tools for in silico analysis of promoter sequences. Nucleic acids research 30 (1), 325–327.
Livak, K.J., Schmittgen, T.D., 2001. Analysis of relative gene expression data using real-time quantitative PCR and the 2(-Delta Delta C(T)) Method. Methods 25 (4), 402–408.
Luna, D.F., Pons, A.B.S., Bustos, D., Taleinik, E., 2018. Early responses to Fe-deficiency distinguish sorghum bicolor genotypes with contrasting alkalinity tolerance. Environ. Exp. Bot. 155, 165–176.
Lutts, S., Kinet, J.M., Bouharmont, J., 1996. NaCl-induced senescence in leaves of rice (*Oryza sativa* L.) cultivar differing in salinity resistance. Ann. Bot. 78, 389–398.
Mimmo, T., Del Buono, D., Terzano, R., Tomasi, N., Vigani, G., Crecchio, R., 2014. Rhizospheric organic compounds in the soil-microorganism-plant system: their role in iron availability. Eur. J. Soil Sci. 65, 629–642.
Mittova, V., Tal, M., Volokita, M., Guy, M., 2003. Up-regulation of the leaf mitochondrial and peroxisomal antioxidative systems in response to salt-induced oxidative stress in the wild salt-tolerant tomato species Lycopersicon pennellii. Plant Cell Environ. 26, 845–856.
Nikolic, D.B., Nesic, S., Bosnic, D., Kostic, L., Nikolic, M., Samardzic, J.T., 2019. Silicon alleviates iron deficiency in barley by enhancing expression of strategy II genes and metal redistribution. Front Plant Sci. 10, 416.
Obour, A., Schlegel, A., Perumal, R., Holman, J., Riaz, D.R., 2019. Evaluating grain sorghum hybrids for tolerance to iron chlorosis. J. Plant Nutr. 42, 401–409.
Pearce, S., Tabbita, F., Cantu, D., Buffalo, V., Avni, R., Vazquez-Gross, H., Zhao, R., Conley, C.J., Distelfeld, A., Dubocovksy, J., 2014. Regulation of Zn and Fe transporters by the GPC1 gene during early wheat monocarpic senescence. BMC Plant Biol. 14, 368.
Ramírez, L., Bartoli, C.G., Lamattina, L., 2013. Glutathione and ascorbic acid protect Arabidopsis plants against detrimental effects of iron deficiency. J. Exp. Bot. 64, 3169–3178.
Ranieri, A., Castagna, A., Soldatini, G.F., 2000. Iron deficiency induces variations in oxidative stress bioindicators in sunflower plants. Agricol. Mediter. 129, 180–192.
Römheld, V., Marschner, H., 1990. Genotypical differences among graminaceous species in release of phytosiderophores and uptake of iron phytosiderophores. In: Genetic Aspects of Plant Mineral Nutrition. Springer, pp. 77–83.
Schmidt, S.B., Pedas, P., Laursen, K.H., Schjoerring, J.K., Husted, S., 2013. Latent manganese deficiency in barley can be diagnosed and remediated on the basis of chlorophyll a fluorescence measurements. Plant Soil 372, 417–442.
Sharma, S., 2007. Adaptation of photosynthesis under iron deficiency in maize. J. Plant Physiol. 164 (10), 1261–1267.
Stocking, C.R., 1975. Iron Deficiency and the Structure and Physiology of Maize Chloroplasts. Plant Physiol. 55 (4), 626–631.
Sun, M., Zigman, S., 1978. An improved Spectrophotomeric assay for Superoxide dismutase based on epinephrine autoxidation. Anal. Biochem. 90, 81–89.
Takahashi, M., Terada, Y., Nakai, I., Nakanishi, H., Yoshimura, E., Mori, S., Nishizawa, N.K., 2003. Role of nicotianamine in the intracellular delivery of metals and plant reproductive development. Plant Cell 15, 1263–1280.
Vert, G., Grotz, N., Dédaldéchamp, F., Gaymard, F., Guerinot, M.L., Briat, J.-F., Curie, C., 2002. *IRT1*, an Arabidopsis transporter essential for iron uptake from the soil and for plant growth. Plant Cell 14, 1223–1233.
Vigani, G., Maffi, D., Zocchi, G., 2009. Iron availability affects the function of mitochondria in cucumber roots. New Phytol. 182, 127–136.
Wang, M., Kawakami, Y., Bhullar, N.K., 2019. Molecular analysis of iron deficiency response in hexaploid wheat. Front. Sust. Food Syst. 3, 67.
Wang, M.-Y., Xia, R.-X., Hu, L.-M., Dong, T., Wu, Q.-S., 2007. Arbuscular mycorrhizal fungi alleviate iron deficient chlorosis in Poncirus trifoliata L. Raf under calcium bicarbonate stress. J. Hort. Sci. Biotech. 82, 776–780.
Yang, Y., Han, X., Liang, Y., Ghosh, A., Chen, J., Tang, M., 2015. The combined effects of arbuscular mycorrhizal fungi (AMF) and lead (Pb) stress on Pb accumulation, plant growth parameters, photosynthesis, and antioxidant enzymes in *Robinia pseudoacacia* L. PLoS One 10, e0145726.
Yordem, B.K., Conte, S.S., Ma, J.F., Yokosho, K., Vasques, K.A., Gopalsamy, S.N., Walker, E.L., 2011. Brachypodium distachyon as a new model system for understanding iron homeostasis in grasses: phylogenetic and expression analysis of Yellow Stripe-Like (YSL) transporters. Ann. Bot. 108, 821–833.
Zhang, X., Zhang, D., Sun, W., Wang, T., 2019. The Adaptive mechanism of plants to iron deficiency via iron uptake, transport, and homeostasis. Int. J Mol. Sci 20, 2424.
Zhao, J., Fujita, K., Sakai, K., 2005. Oxidative stress in plant cell culture: a role in production of β-thujaplicin by Cupressus lusitanica cell cultures. Biotech. Bioeng. 90, 621–631.
Zuchi, S., Watanabe, M., Hubberten, H.M., Bromke, M., Osorio, S., Fernie, A.R., Celletti, S., Paolacci, A.R., Catarcione, G., Ciaffi, M., Hoefgen, R., Astolfi, S., 2015. The interplay between sulfur and iron nutrition in tomato. Plant Physiol. 169 (4), 2624–2639.
Zuchi, S., Cesco, S., Varanini, Z., Pinton, R., Astolfi, S., 2009. Sulphur deprivation limits Fe-deficiency responses in tomato plants. Planta 230, 85–94.